Monthly Notices
of the
ROYAL ASTRONOMICAL SOCIETY

MNRAS **440,** 75–88 (2014)
Advance Access publication 2014 March 7

doi:10.1093/mnras/stu259

Cosmic degeneracies – I. Joint *N*-body simulations of modified gravity and massive neutrinos

Marco Baldi,[1,2,3]★ Francisco Villaescusa-Navarro,[4] Matteo Viel,[4,5] Ewald Puchwein,[6,7] Volker Springel[7,8] and Lauro Moscardini[1,2,3]

[1]*Dipartimento di Fisica e Astronomia, Alma Mater Studiorum Università di Bologna, viale Berti Pichat, 6/2, I-40127 Bologna, Italy*
[2]*INAF – Osservatorio Astronomico di Bologna, via Ranzani 1, I-40127 Bologna, Italy*
[3]*INFN – Sezione di Bologna, viale Berti Pichat 6/2, I-40127 Bologna, Italy*
[4]*INAF – Osservatorio Astronomico di Trieste, Via Tiepolo 11, I-34143 Trieste, Italy*
[5]*INFN/National Institute for Nuclear Physics, Via Valerio 2, I-34127 Trieste, Italy*
[6]*Institute of Astronomy and Kavli Institute for Cosmology, University of Cambridge, Madingley Road, Cambridge CB3 0HA, UK*
[7]*Heidelberger Institut für Theoretische Studien (HITS), Schloss-Wolfsbrunnenweg 35, D-69118 Heidelberg, Germany*
[8]*Zentrum für Astronomie der Universität Heidelberg, ARI, Mönchhofstrasse 12-14, D-69120 Heidelberg, Germany*

Accepted 2014 February 6. Received 2014 February 5; in original form 2013 November 11

ABSTRACT

We present the first suite of cosmological *N*-body simulations that simultaneously include the effects of two different and theoretically independent extensions of the standard Λ cold dark matter (ΛCDM) cosmological scenario – namely an $f(R)$ theory of modified gravity and a cosmological background of massive neutrinos – with the aim to investigate their possible observational degeneracies. We focus on three basic statistics of the large-scale matter distribution, more specifically the non-linear matter power spectrum, the halo mass function, and the halo bias. Our results show that while these two extended models separately determine very prominent and potentially detectable features in all the three statistics, when we allow them to be simultaneously at work these features are strongly suppressed. In particular, when an $f(R)$ gravity model with $f_{R0} = -1 \times 10^{-4}$ is combined with a total neutrino mass of $\Sigma_i m_{\nu_i} = 0.4$ eV, the resulting matter power spectrum, halo mass function, and bias at $z = 0$ are found to be consistent with the standard model's predictions at the $\lesssim$10, $\lesssim$20, and $\lesssim$5 per cent accuracy levels, respectively. Therefore, our results imply an intrinsic theoretical limit to the effective discriminating power of present and future observational data sets with respect to these widely considered extensions of the standard cosmological scenario.

Key words: galaxies: formation – cosmology: theory – dark energy – dark matter.

1 INTRODUCTION

The primary scientific goal of a wide range of present and future observational initiatives in the field of cosmology – such as e.g. BOSS (Ahn et al. 2013), PanStarrs (Kaiser et al. 2002), HETDEX (Hill et al. 2008), DES (Abbott et al. 2005), LSST (Ivezic et al. 2008), and *Euclid*[1] (Laureijs et al. 2011) – consists in combining different probes of the geometric and dynamical evolution of the Universe to unveil possible deviations from the expected behaviour of the standard Λ cold dark matter (ΛCDM) cosmological scenario. The latter relies on the assumption of a cosmological constant Λ as the source of the observed accelerated expansion of the Universe (Riess et al. 1998; Schmidt et al. 1998; Perlmutter et al. 1999) and on the existence of some yet undetected CDM particles with negligible non-gravitational interactions that could enhance the growth of cosmic structures from the tiny density perturbations observed in the primordial Universe through detailed cosmic microwave background (CMB) observations (see e.g. Smoot et al. 1992; Ade et al. 2013; Bennett et al. 2013) to the highly structured Universe that we observe today (see e.g. Abazajian et al. 2009).

Although the standard ΛCDM cosmological model has so far been found to be consistent with observational data at ever increasing levels of accuracy (see e.g. Blake et al. 2011; Ade et al. 2013), its theoretical foundations remain poorly motivated in the absence of a clear understanding of the physical origin of the cosmological constant Λ and of a direct (or indirect) detection of the elementary particle associated with CDM. This lack of a firm theoretical and observational basis for the standard ΛCDM picture has motivated the exploration of a large number of alternative scenarios both concerning the origin of the accelerated expansion and the nature of the CDM cosmic field.

★ E-mail: mail@marcobaldi.it
[1] www.euclid-ec.org

The former range of extended models includes on one hand generalized dark energy (DE) scenarios where the cosmic acceleration is driven by a classical scalar field (see e.g. Ratra & Peebles 1988; Wetterich 1988; Armendariz-Picon, Mukhanov & Steinhardt 2001; Caldwell 2002; Feng, Wang & Zhang 2005) possibly characterized by non-trivial clustering (see e.g. Creminelli et al. 2009; Sefusatti & Vernizzi 2011; Batista & Pace 2013) or interaction (see e.g. Wetterich 1995; Amendola 2000; Farrar & Peebles 2004; Amendola, Baldi & Wetterich 2008; Baldi 2011) properties, and on the other hand, several possible modified gravity (MG) models including *scalar–tensor theories* of gravity [such as e.g. $f(R)$ models, Buchdahl 1970; Starobinsky 1980; Hu & Sawicki 2007; Sotiriou & Faraoni 2010], the *DGP* scenario (Dvali, Gabadadze & Porrati 2000), or the *Galileon* model (Nicolis, Rattazzi & Trincherini 2009). In this work, we will focus on the second class of extensions of the standard cosmology, and in particular on the widely investigated parametrization of $f(R)$ theories of gravity proposed by Hu & Sawicki (2007).

The latter range of models, instead, includes various extensions of the CDM paradigm characterized by different assumptions on the nature of the fundamental dark matter particle, both concerning its phase-space distribution – as for the case of warm dark matter models (see e.g. Bode, Ostriker & Turok 2001; Viel et al. 2013) or mixed dark matter scenarios (Maccio' et al. 2012) – and its interaction properties (see e.g. Loeb & Weiner 2011; Baldi 2013). While the fundamental composition of the dark matter fraction of the total cosmic energy budget has very little impact on the background expansion history of the universe, it can significantly affect the growth of density perturbations both in the linear and in the non-linear regimes. In particular, one of the most significant extensions of the standard cosmological scenario for what concerns the structure formation processes amounts to dropping the assumption of massless neutrinos that is commonly adopted in both analytical and numerical investigations of the late-time universe. The discovery of the neutrino oscillation phenomena (Cleveland et al. 1998) has revealed in an unambiguous way that at least two of the three neutrino families are massive, such that a fraction of the total matter density of the Universe *must* be associated with the cosmic neutrino background. In this respect, the inclusion of massive neutrinos into any cosmological scenario should no longer be regarded as one (amongst many) possible extension of the basic standard model into the realm of exotic physics, but rather as a necessary ingredient in order to faithfully reproduce reality. As such, any realistic cosmological modelling – both for the standard cosmological constant Λ and for alternative DE or MG scenarios – should no longer avoid to properly take into account the possibility that part of the dark matter energy density be made of non-relativistic massive neutrinos.

In recent years, significant progress has been made in including the effects of massive neutrinos into cosmological N-body codes employed to study structure formation processes from the linear to the highly non-linear regime in the context of standard ΛCDM cosmologies (see e.g. Brandbyge et al. 2008; Brandbyge & Hannestad 2009; Brandbyge & Hannestad 2010; Viel, Haehnelt & Springel 2010; Agarwal & Feldman 2011; Bird, Viel & Haehnelt 2012; Wagner, Verde & Jimenez 2012). Here, by 'standard ΛCDM cosmologies' we refer to models where the accelerated cosmic expansion is driven by a cosmological constant and where a fixed total matter density is made up by a fraction of standard CDM particles and by a fraction of massive neutrinos. Such works have highlighted a number of effects that appreciably modify observable quantities (such as e.g. the non-linear matter power spectrum, the abundance of collapsed haloes as a function of their mass, the pattern of redshift-space distortions, or the clustering properties of dark matter haloes, see e.g. Viel et al. 2010; Marulli et al. 2011; Castorina et al. 2013; Villaescusa-Navarro et al. 2013a, respectively) in massive neutrinos cosmologies as compared to their massless neutrinos counterparts, thereby possibly biasing the inference of cosmological parameters from these observables. Similarly, significant progress has been made in implementing alternative DE and MG models in N-body algorithms (see e.g. Baldi 2012 for a recent review), which have allowed self-consistent cosmological simulations in the context of a wide range of such non-standard scenarios for the accelerated cosmic expansion. However, no attempt has been made so far to combine such two efforts and investigate the effects of massive neutrinos on the formation and evolution of linear and non-linear cosmic structures in the context of alternative DE and MG models.

In this paper – which is the first in a series of works aimed at studying the intrinsic observational degeneracies between different and independent extensions of the standard ΛCDM scenario – we attempt for the first time to investigate the joint effects of $f(R)$ MG theories and massive neutrinos in the non-linear regime of structure formation by means of a specifically designed N-body code that is capable of simultaneously including both these additional ingredients in its integration scheme. The latter is a modified version of the widely used TreePM N-body code GADGET (Springel 2005) which has been obtained by combining the MG-GADGET implementation of $f(R)$ theories recently developed by Puchwein, Baldi & Springel (2013) with the massive neutrinos module by Viel et al. (2010).

With such code in hand, we have performed for the first time a series of combined simulations for one specific realization of $f(R)$ MG with different amounts of massive neutrinos and compared the outcomes of our runs in terms of some basic statistics of the large-scale structure (LSS) distribution to the same set of neutrino masses acting within a standard ΛCDM cosmology. This work therefore extends the earlier studies of He (2013) and Motohashi, Starobinsky & Yokoyama (2013) to the fully non-linear regime of structure formation. Our results highlight a very strong degeneracy between $f(R)$ MG models and massive neutrinos in all the observables that we have considered, such that a suitable combination of $f(R)$ parameters and neutrino masses might be hardly distinguishable from the standard cosmological scenario even when the two separate effects would result in a very significant deviation from the reference cosmology. This degeneracy should be properly taken into account when assessing the effective discriminating power of present and future observational surveys with respect to individual extensions of the standard cosmological model.

This paper is organized as follows. In Section 2, we introduce the $f(R)$ MG models considered in our numerical simulations. In Section 3, we review the basics of massive neutrinos and their role in cosmological structure formation. In Section 4, we describe the numerical setup of our cosmological simulations and of the initial conditions generation. In Section 5, we present our results on the non-linear matter power spectrum, the halo mass function (HMF), and the halo bias. Finally, in Section 6, we draw our conclusions.

2 $F(R)$ MODIFIED GRAVITY

In this work, we will consider MG cosmologies in the form of $f(R)$ extensions of Einstein's general relativity (hereafter GR). Such models are characterized by the action

$$S = \int \mathrm{d}^4x \sqrt{-g} \left(\frac{R + f(R)}{16\pi G} + \mathcal{L}_\mathrm{m} \right), \quad (1)$$

where the Ricci scalar R that appears in the standard Einstein–Hilbert action of GR has been replaced by $R + f(R)$. In equation (1), G is Newton's gravitational constant, $\mathcal{L}_{\rm m}$ is the Lagrangian density of matter, and g is the determinant of the metric tensor $g_{\mu\nu}$. These models have been widely investigated in the literature, both in terms of their theoretical predictions at linear (see e.g. Pogosian & Silvestri 2008) and non-linear (see e.g. Oyaizu, Lima & Hu 2008; Schmidt et al. 2009; Li et al. 2012a; Puchwein et al. 2013; Llinares, Mota & Winther 2013) scales, and in terms of possible present (see e.g. Lombriser et al. 2012) and forecasted future (Zhao et al. 2009) observational constraints. Within such framework, the quantity $f_R \equiv {\rm d}f(R)/{\rm d}R$ represents an additional scalar degree of freedom obeying an independent dynamic equation that in the quasi-static approximation and in the limit $f_R \ll 1$ takes the form[2] (see again Hu & Sawicki 2007)

$$\nabla^2 f_R = \frac{1}{3}\left(\delta R - 8\pi G\delta\rho\right), \tag{2}$$

where δR and $\delta\rho$ are the perturbations in the scalar curvature and matter density, respectively.

Within the range of possible functional forms of $f(R)$, we will focus on the specific realization proposed by Hu & Sawicki (2007) which has the advantage of providing a close match to the standard ΛCDM background expansion history. In this model, the function $f(R)$ takes the form

$$f(R) = -m^2\frac{c_1\left(\frac{R}{m^2}\right)^n}{c_2\left(\frac{R}{m^2}\right)^n + 1}, \tag{3}$$

where $m^2 \equiv H_0^2\Omega_{\rm M}$, with H_0 being the present-day Hubble parameter and $\Omega_{\rm M}$ the dimensionless matter density parameter defined as the ratio between the mean matter density and the critical density of the universe, and c_1, c_2, and n are non-negative constant free parameters that fully specify the model. By imposing the condition $c_2(R/m^2)^n \gg 1$, equation (3) becomes $f(R) = -m^2c_1/c_2 + O((m^2/R)^n)$. It is then possible to obtain a background evolution close to that of a ΛCDM model by setting the term $-m^2c_1/c_2$ equal to -2Λ, where Λ is the desired cosmological constant, which is equivalent to imposing a relation between the two free parameters c_1 and c_2:

$$\frac{c_1}{c_2} = 6\frac{\Omega_\Lambda}{\Omega_{\rm M}}, \tag{4}$$

where $\Omega_\Lambda \equiv \Lambda/3H_0^2$ is the present dimensionless density parameter of the cosmological constant. Under these assumptions, the scalar degree of freedom f_R takes the approximate form:

$$f_R \approx -n\frac{c_1}{c_2^2}\left(\frac{m^2}{R}\right)^{n+1}. \tag{5}$$

By evaluating the present average scalar curvature of the universe $\bar{R}_0$ within a standard ΛCDM cosmology and combining with equation (5), one gets an equation for the background value of the present scalar degree of freedom $\bar{f}_{R0}$. Then, by fixing the value of $\bar{f}_{R0}$, it is possible to obtain an independent relation between c_1 and c_2 as a function of n, which combined with equation (4) completely determines both parameters. Therefore, the model can be fully specified by fixing n and $\bar{f}_{R0}$ rather than c_1 and c_2. Following the convention adopted in most of the literature, we will stick to the former choice throughout the rest of the paper.

[2] Whenever not explicitly stated otherwise, we always work in units where the speed of light is assumed to be unity, $c = 1$.

The above equations further simplify after fixing the value of n, which is set to unity in all the cosmological realizations presented in this work. For $n = 1$, then, the model is fully specified by the single parameter $\bar{f}_{R0}$, and the time evolution of the background scalar degree of freedom $\bar{f}_R$ is given by

$$\bar{f}_R(a) = \bar{f}_{R0}\left(\frac{\bar{R}_0}{\bar{R}(a)}\right)^2 = \bar{f}_{R0}\left(\frac{1 + 4\frac{\Omega_\Lambda}{\Omega_{\rm M}}}{a^{-3} + 4\frac{\Omega_\Lambda}{\Omega_{\rm M}}}\right)^2, \tag{6}$$

while the curvature perturbation takes the form

$$\delta R = \bar{R}(a)\left(\sqrt{\frac{\bar{f}_R(a)}{f_R}} - 1\right). \tag{7}$$

In $f(R)$ models, the gravitational potential Φ satisfies (Hu & Sawicki 2007)

$$\nabla^2\Phi = \frac{16\pi G}{3}\delta\rho - \frac{1}{6}\delta R, \tag{8}$$

where the second term on the right-hand side is responsible for the spatial dependence of the fifth-force arising as a consequence of the modification of the laws of gravity in addition to the standard Newtonian force. To carry out our analysis, we will resort to the MG-GADGET implementation (Puchwein et al. 2013) of $f(R)$ models into the widely used parallel TREE-PM N-body code GADGET3 that will be briefly described in Section 4. This numerical tool allows us to solve equation (2) for a generic density distribution given by a set of N-body particles and then to compute the total force arising on each particle through equation (8), by including in the source term the curvature perturbation δR obtained according to equation (7). We refer the interested reader to the MG-GADGET code paper for a more detailed presentation of the numerical implementation.

3 MASSIVE NEUTRINOS AND STRUCTURE FORMATION

Neutrinos were initially postulated in 1930 by Pauli as a solution to the apparent violation of energy, momentum and spin conservation in the β-decay process. In 1956, their existence was corroborated for the first time in the famous experiment carried out by Cowan & Reines (Cowan et al. 1956). The measurements of the Z boson lifetime have then pointed out that the number of light neutrino families is 3. Moreover, since the discovery of the neutrino oscillation phenomena (Cleveland et al. 1998) it is known that at least two of the three neutrino families are massive, in contrast to the particle standard model assumption. Whereas measuring the absolute masses of the neutrinos is very difficult, the neutrino oscillations can be used to measure the mass square differences among the neutrino mass eigenstates. The most recent measurements from solar, atmospheric, and reactor neutrinos result in $\triangle m^2_{12} = 7.5 \times 10^{-5}$ eV^2 and $|\triangle m^2_{23}| = 2.3 \times 10^{-3}$ eV^2 (Fogli et al. 2012; Forero, Tórtola & Valle 2012, respectively), with m_1, m_2, and m_3 being the masses of the three neutrino mass eigenstates. Unfortunately, the experimental measurements do not allow us to determine the sign of the quantity $\triangle m^2_{23}$. This gives rise to two different possible mass orderings (or hierarchies): the *normal* hierarchy, where $m_1 < m_2 < m_3$, and the *inverted* hierarchy, where $m_3 < m_1 < m_2$.

Knowing the absolute masses of the neutrinos is of critical importance, since they represent a door to look for physics beyond the standard model. Whereas the neutrino oscillations have been used to set lower limits on the sum of the neutrino masses, $\Sigma_i m_{\nu_i} \geq 0.056$ and 0.095 eV for the normal and inverted hierarchies, respectively,

the tighter upper bounds on the masses of the neutrinos come from cosmological observations.

In the very early universe, neutrinos were in thermal equilibrium with the photons, the electrons and then the positrons, while in thermal equilibrium, their momentum distribution followed the standard Fermi–Dirac distribution. Then, it is easy to show that once neutrinos decouple from the primordial plasma, their momentum distribution follows

$$n(p)\,\mathrm{d}\,p = \frac{4\pi g_\nu}{(2\pi\hbar c)^3}\frac{p^2\mathrm{d}p}{\mathrm{e}^{\frac{p}{k_B T_\nu}}+1}, \tag{9}$$

where $n(p)$ is the number of cosmic neutrinos with momentum between p and $p + \mathrm{d}p$, g_ν is the number of neutrino spin states, and k_B is the Boltzmann constant. The temperatures of the cosmic neutrino background and that of the CMB are related by $T_\nu(z = 0) = \left(\frac{4}{11}\right)^{1/3} T_\gamma(z = 0)$ (see for instance Weinberg 2008) such that the temperature of the neutrino cosmic background at redshift z is given by $T_\nu(z) \cong 1.95(1 + z)$ K. The current abundance of relic neutrinos, obtained by integrating equation (9), results in 113 neutrinos per cubic centimetre per neutrino family. The fraction of the total energy density of the universe made up by massive neutrinos can also be easily derived from equation (9):

$$\Omega_\nu = \frac{\Sigma_i m_{\nu_i}}{93.14h^2\,\mathrm{eV}}. \tag{10}$$

During the radiation-dominated era, neutrinos constituted an important fraction of the total energy density of the universe, playing a crucial role in setting the abundance of the primordial elements. The impact of massive neutrinos on cosmology is very well understood at the linear order (Lesgourgues & Pastor 2006): on one hand, massive neutrinos modify the matter–radiation equality time, and on the other hand, they slow down the growth of matter perturbations. The combination of the above two effects produces a suppression on the matter power spectrum at small scales (see for instance Lesgourgues & Pastor 2006). The signatures left by neutrino masses on both the matter power spectrum and the CMB have been widely used to set upper limits on their masses. Different studies point out that $\Sigma_i m_{\nu_i} < 0.3$ eV with a confidence level of 2σ (Joudaki 2012; Riemer-Sorensen et al. 2012; Xia et al. 2012; Ade et al. 2013; Zhao et al. 2013).

Even though the impact of neutrino masses is well understood at the linear order, the impact of massive neutrinos on the fully non-linear regime has so far received little attention. Recent studies using N-body simulations with massive neutrinos have investigated the neutrino imprints on the non-linear matter power spectrum (Brandbyge et al. 2008; Brandbyge & Hannestad 2009; Brandbyge & Hannestad 2010; Viel et al. 2010; Agarwal & Feldman 2011; Bird et al. 2012; Wagner et al. 2012). Such studies have pointed out that in the fully non-linear regime massive neutrinos induce a scale- and redshift-dependent suppression on the matter power spectrum which can be up to ∼25 per cent larger than the predictions of the linear theory.

The mean thermal velocity of the cosmic neutrinos, obtained from equation (9), is given by $\sim 160(1 + z)\frac{\mathrm{eV}}{m_\nu}$ km s^{-1}. For neutrinos with $\Sigma_i m_{\nu_i} = 0.3$ eV, their mean velocity today is then ∼500 km s^{-1}, i.e. low enough to cluster within the gravitational potential wells of galaxy clusters. The neutrino clustering has been studied in several works (Singh & Ma 2003; Ringwald & Wong 2004; Brandbyge et al. 2010; Villaescusa-Navarro et al. 2011a, 2013a). In Villaescusa-Navarro et al. (2011a), for instance, the authors studied the possibility of detecting the excess of mass in the outskirts of galaxy clusters due to the extra mass contribution arising from the clustering of massive neutrinos. Furthermore, in Villaescusa-Navarro et al. (2013a), it was shown that the neutrino clustering also affects the shape and amplitude of the neutrino momentum distribution of equation (9) at low redshift.

Massive neutrinos also leave their imprint on the HMF. In the pioneering work of Brandbyge et al. (2010), the authors computed the HMF in cosmologies with massive neutrinos using N-body simulations. They compared their results with the HMF obtained by using the Sheth–Tormen HMF and found that reasonable agreement between the results of the N-body simulations and the Sheth–Tormen HMF (Sheth & Tormen 1999) was achieved if the latter was computed using the total matter power spectrum but the mean CDM density of the universe, ρ_CDM. These findings were subsequently corroborated by Villaescusa-Navarro et al. (2013a) and Marulli et al. (2011). However, in the recent work by Ichiki & Takada (2012), it was suggested that an even better agreement would be obtained by using the linear CDM power spectrum instead of the total matter linear power spectrum. This claim has been tested against N-body simulations resulting in an excellent agreement (see e.g. Castorina et al. 2013; Costanzi et al. 2013). Moreover, in Castorina et al. (2013), it was shown that this is the only way of parametrizing the HMF in an almost universal form, i.e. independently of the underlying cosmological model.

The impact of neutrino masses on the LSS of the universe covers a wide range of aspects. In Villaescusa-Navarro et al. (2011b), it was suggested that massive neutrinos could play an important role in the dynamics of cosmological voids. The reason is that the large thermal velocities of the neutrinos make them less sensitive to the gravitational evolution of voids. In other words, one would naively expect cosmic voids to be empty of CDM, but not of cosmological neutrinos. The contribution of neutrinos to the void's total mass has then important consequences in terms of its evolution. Villaescusa-Navarro et al. (2011b) used such argument to study the possible signature left by massive neutrinos on Lyman α voids.

In a series of recent papers (Castorina et al. 2013; Villaescusa-Navarro et al. 2013b), it has also been shown that on large scales the bias between the spatial distribution of dark matter haloes and that of the underlying matter exhibits a dependence on scale for cosmological models with massive neutrinos. Such scale dependence is highly suppressed if the bias is computed with respect to the spatial distribution of the CDM instead of the total matter.

As briefly summarized in the present section, the effects induced by massive neutrinos on the LSS of the universe are numerous. In this work, we further explore such effects in non-standard cosmologies. More specifically, we study the combined effects on structure formation of a cosmic background of massive neutrinos with different values of the total neutrino mass and of a modification of standard gravity in the form of the $f(R)$ gravitational action introduced in equation (1). The main aim of this work is therefore to investigate whether the simultaneous existence of an extended theory of gravity and of a massive neutrino background might impact on the observational capability of detecting and/or constraining any of such two extensions of the standard cosmological scenario. Then, as will become clear in the rest of the paper, the upper bounds on the total neutrino mass quoted in the present section that have been obtained through cosmological observations might not be valid anymore if the underlying theory of gravity is different from standard GR. Analogously, present and future constraints on the nature of gravity might be strongly biased in the presence of a significant massive neutrino background.

Table 1. The suite of cosmological *N*-body simulations considered in this work, with their main physical and numerical parameters. Here, $\Omega_{\rm CDM}$ and Ω_ν indicate the energy density ratio to the critical density of the universe for CDM and neutrinos, respectively, while $M^p_{\rm CDM}$ and M^p_ν stand for the mass of CDM and neutrino particles in the different *N*-body runs.

Run	Theory of gravity	$\Sigma_i m_{\nu_i}$ (eV)	$\Omega_{\rm CDM}$	Ω_ν	$M^p_{\rm CDM}$ ($\rm M_\odot\, h^{-1}$)	M^p_ν ($\rm M_\odot\, h$)
GR-nu0	GR	0	0.3175	0	6.6×10^{11}	0
GR-nu0.2	GR	0.2	0.3127	0.0048	6.47×10^{11}	9.86×10^{9}
GR-nu0.4	GR	0.4	0.308	0.0095	6.4×10^{11}	1.97×10^{10}
GR-nu0.6	GR	0.6	0.3032	0.0143	6.27×10^{11}	2.96×10^{10}
fR-nu0	$\bar{f}_{R0} = -1 \times 10^{-4}$	0	0.3175	0	6.6×10^{11}	0
fR-nu0.2	$\bar{f}_{R0} = -1 \times 10^{-4}$	0.2	0.3127	0.0048	6.47×10^{11}	9.86×10^{9}
fR-nu0.4	$\bar{f}_{R0} = -1 \times 10^{-4}$	0.4	0.308	0.0095	6.4×10^{11}	1.97×10^{10}
fR-nu0.6	$\bar{f}_{R0} = -1 \times 10^{-4}$	0.6	0.3032	0.0143	6.27×10^{11}	2.96×10^{10}

4 COSMOLOGICAL SIMULATIONS

The aim of this work is to investigate the joint effects of MG and massive neutrinos on the basic statistical properties of structure formation, like the non-linear matter power spectrum, the HMF, and the large-scale halo bias, with the goal of quantifying the level of degeneracy between these two independent extensions of the standard cosmological scenario that is usually adopted for large *N*-body simulations, i.e the ΛCDM cosmology with massless neutrinos. Furthermore, we aim to assess the discriminating power of present and future observational data with respect to such extended cosmologies. In order to include in our comparison both the linear and non-linear regimes of structure formation to investigate whether a suitable combination of such different regimes might help in breaking – or at least alleviating – possible degeneracies, we need to rely on dedicated *N*-body simulations that include at the same time the effects of $f(R)$ modifications of gravity and of a cosmic neutrino background with different possible values of the total neutrino mass $\Sigma_i m_{\nu_i}$. To this end, we have combined the MG-GADGET implementation of $f(R)$ models by Puchwein et al. (2013) with the massive neutrinos module developed by Viel et al. (2010), both included in the widely used TREE-PM *N*-body code GADGET3. More specifically, the simulations presented in this work are based on explicitly modelling the neutrinos with particles, as opposed to adopting the approximate Fourier-based technique (where they are added as an extra force in *k*-space). Using particles has the disadvantage of having significant Poisson noise in the neutrino density field, but it is ultimately the more general technique capable of accounting correctly for all non-linear effects. Furthermore, our numerical setting ensures that noise issues are unimportant in the regime that we are analysing. The combination of these two different modules has required some changes to the original independent implementations in order to allow the handling of very high memory allocation requirements arising when applying the multigrid acceleration scheme of MG-GADGET (see again Puchwein et al. 2013 for a detailed description of the multigrid scheme) to two particle species with very different spatial distributions.

With such combined *N*-body code at hand, we have performed a suite of intermediate-resolution *N*-body simulations on a periodic cosmological box of 1 $\rm Gpc\, h^{-1}$ aside filled with an equal number $N = 512^3$ of CDM and neutrino particles, for a range of different cosmological models characterized by two possible theories of gravity – namely standard GR and $f(R)$ with $n = 1$ and $\bar{f}_{R0} = -1 \times 10^{-4}$ – and different values of the total neutrino masses $\Sigma_i m_{\nu_i} = \{0\,, 0.2\,, 0.4\,, 0.6\}$ eV. The full range of cosmologies covered by our simulations suite is summarized in Table 1. All runs are carried out using the latest *Planck* constraints (Ade et al. 2013) on the background cosmological parameters, which are summarized in the upper part of Table 2, and on the amplitude $\mathcal{A}_{\rm s}$ and spectral index n_s of the linear matter power spectrum at $z_{\rm CMB} \approx 1100$ (listed in the bottom part of Table 2), thereby resulting in slightly different values of $\sigma_8(z = 0)$ for the different cosmologies.

Table 2. The set of cosmological parameters adopted in this work, consistent with the latest results of the Planck Collaboration (Ade et al. 2013). Here, $n_{\rm s}$ is the spectral index of primordial density perturbations, while $\mathcal{A}_{\rm s}$ is the amplitude of scalar perturbations at the redshift of the CMB.

Parameter	Value
H_0	67.1 km $\rm s^{-1}$ $\rm Mpc^{-1}$
$\Omega_{\rm M}$	0.3175
$\Omega_{\rm DE}$	0.6825
$\Omega_{\rm b}$	0.049
$\mathcal{A}_{\rm s}$	2.215×10^{-9}
$n_{\rm s}$	0.966

Initial conditions have been generated with a modified version of the widely used N-GENIC code that allows us to include an additional matter component – besides the standard CDM and gas particle types – with the density perturbations and the thermal velocity distribution of a cosmic neutrino background as computed by the public Boltzmann code CAMB[3] (Lewis, Challinor & Lasenby 2000) for any given total neutrino mass $\Sigma_i m_{\nu_i}$. In particular, the initial conditions were generated at $z = 99$ by perturbing the positions of the CDM and neutrino particles, which were set initially into a cubic regular grid, using the Zel'dovich approximation. The linear matter power spectra employed to set up initial conditions for the various total neutrino masses are displayed in Fig. 1, along with the ratio to the fiducial massless neutrino case. Since at such high redshift the MG fifth-force is fully screened, for each total neutrino mass we used the same initial conditions for both the GR and the $f(R)$ simulations.

We incorporate the effects of baryons by using a transfer function that is a weighted average of the CDM and baryon transfer functions as given by CAMB, even if in the present simulations we do not include baryonic particles as a separate species in the *N*-body runs.

[3] www.cosmologist.info

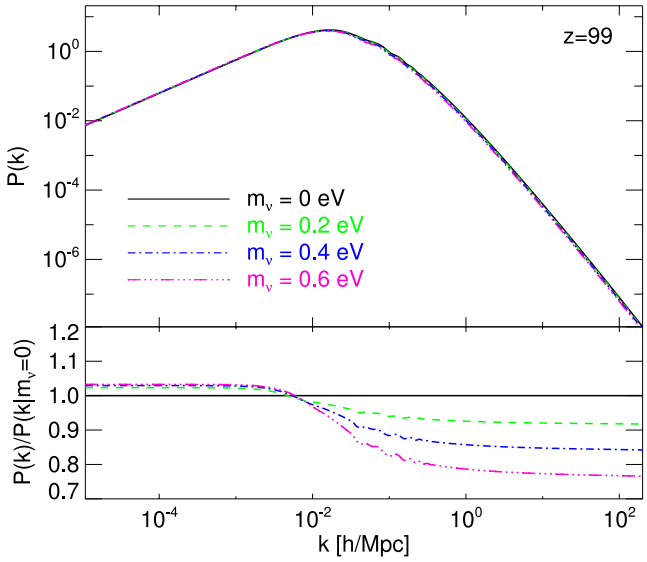

Figure 1. The linear matter power spectra adopted for the initial conditions of the simulations with different total neutrino mass.

The neutrino particles also receive an extra velocity component arising from random sampling the neutrino momentum distribution at the starting redshift. In all the different runs, the total matter density is kept fixed at the *Planck* value of $\Omega_{\rm M} = 0.3175$ which is split into the contribution of CDM and massive neutrinos, with the latter being given by equation (10). As a result, the CDM density and the corresponding mass of simulated CDM particles decreases when $\Sigma_i m_{\nu_i}$ is increased, as summarized in Table 1.

5 RESULTS

We now describe the main outcomes of our numerical investigation of combined $f(R)$ and massive neutrinos cosmologies, concerning the non-linear matter power spectrum, the CDM HMF, and the halo-matter bias.

5.1 The non-linear matter power spectrum

For each of our cosmological simulations, we have computed the total (i.e. CDM plus neutrinos) non-linear matter power spectrum by determining the density field on a cubic Cartesian grid with twice the resolution of the PM grid used for the N-body integration (i.e. 1024^3 grid nodes) through a cloud-in-cell mass assignment. This procedure provides a determination of the non-linear matter power spectrum up to the Nyquist frequency of the PM grid, corresponding to $k_{\rm Ny} = \pi N/L \approx 3.2\,h\,{\rm Mpc}^{-1}$. The obtained power spectrum is then truncated at the k-mode where the shot noise reaches 20 per cent of the measured power. With the simulated power spectra, we can estimate the separate effects of $f(R)$ MG and of massive neutrinos on the linear and non-linear regimes of structure formation at different redshifts. Furthermore, we are able to compute for the first time the joint effects of both independent extensions of the standard fiducial cosmological model on the amplitude of linear and non-linear density perturbations.

In Fig. 2, we display the ratio of the non-linear matter power spectrum of standard GR cosmologies with different neutrino masses to the fiducial case of massless neutrinos, for the three different redshifts $z = \{0, 0.6, 1.3\}$. As expected, the massive neutrino component suppresses the power spectrum amplitude both at linear and non-linear scales, with a progressively more significant impact for larger values of the total neutrino mass $\Sigma_i m_{\nu_i}$. This is consistent with numerous previous investigations of structure formation processes in the presence of a massive neutrino component (see e.g.

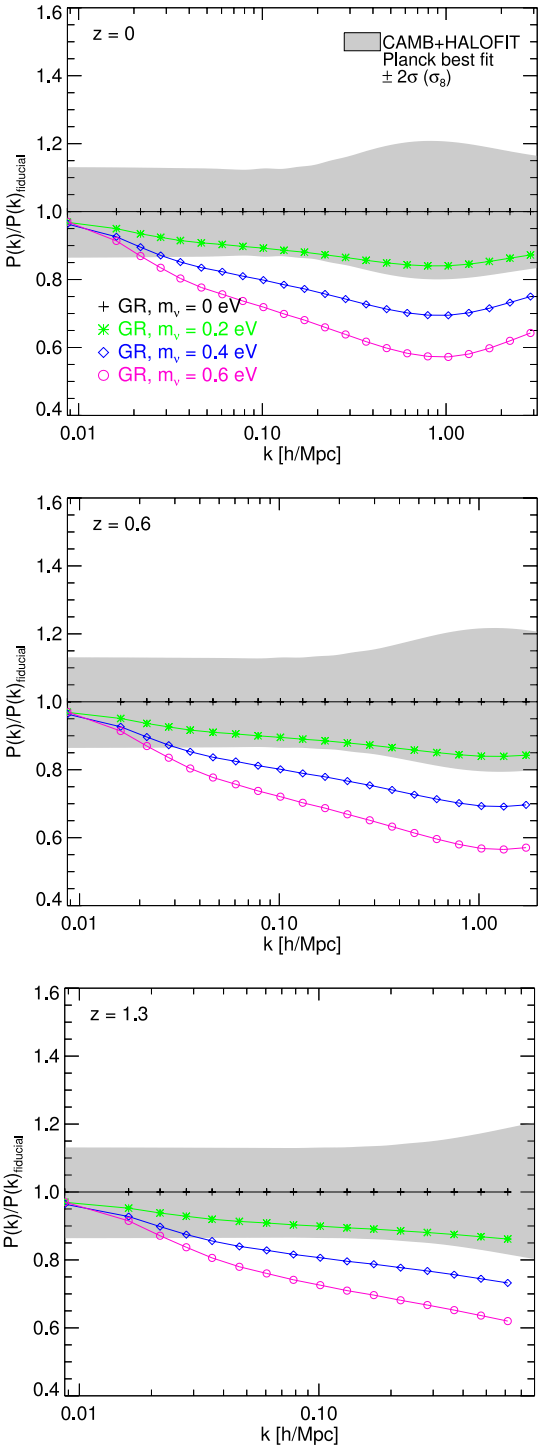

Figure 2. The non-linear matter power spectrum ratio with respect to the fiducial model for different values of the total neutrino mass as labelled. The different panels refer to $z = 0$ (top), $z = 0.6$ (middle), and $z = 1.3$ (bottom). The grey shaded area represents the region obtained with CAMB and HALOFIT by setting all cosmological parameters to their fiducial *Planck* values except σ_8 which is allowed to vary within its 2σ confidence interval.

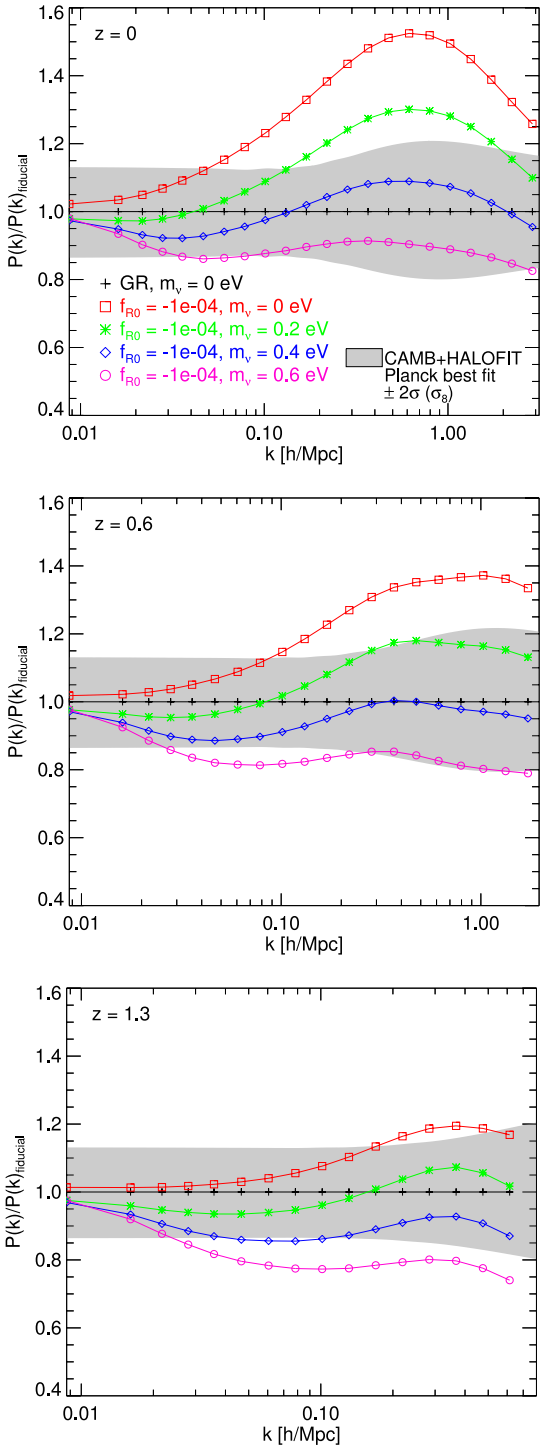

Figure 3. As Fig. 2, but for the combined simulations of $f(R)$ gravity and massive neutrinos.

Brandbyge et al. 2008; Viel et al. 2010; Agarwal & Feldman 2011; Bird et al. 2012; Wagner et al. 2012).

In the uppermost panel of Fig. 3, instead, we show the same power ratio to the fiducial model for the combined simulations of $f(R)$ MG with different neutrino masses at $z = 0$. As one can see in the figure, for the massless neutrino run (red line), the power spectrum ratio shows the typical shape already found by several authors (see e.g. Oyaizu et al. 2008; Li et al. 2012b; Puchwein et al. 2013) for the same $\bar{f}_{R0} = -1 \times 10^{-4}$ MG scenario investigated here, which is characterized by a growing enhancement at linear and mildly non-linear scales that reach a peak of about 50 per cent at $k \sim 0.6\,h\,\mathrm{Mpc}^{-1}$ (at $z = 0$), followed by a decrease at progressively more non-linear scales. The latter decrease is produced by the shift of the transition scale between the one-halo and two-halo term domination in the density power spectrum associated with the effectively larger value of σ_8 in the $f(R)$ cosmology arising at low redshifts as a consequence of the MG fifth-force (see e.g. Zhao, Li & Koyama 2011). Therefore, our pure $f(R)$ run is fully consistent with previous findings for the same cosmological model and with the results of Puchwein et al. (2013) obtained with the MG-GADGET code. The same quantity is displayed in the remaining panels of Fig. 3 for the same redshifts shown in Fig. 2.

One of the main results of this paper is then represented by the remaining curves of Fig. 3, which refer to the impact on the matter power spectrum of different neutrino masses (green, blue, and magenta for $\Sigma_i m_{\nu_i} = 0.2, 0.4, 0.6$ eV, respectively) in the context of an underlying $f(R)$ cosmology. As one can see from the figures, the effect of $f(R)$ on the matter power spectrum is strongly suppressed by the presence of massive neutrinos such that the MG cosmology with neutrino masses of $\Sigma_i m_{\nu_i} = 0.4$ eV does not deviate more than $\approx$10 per cent (at $z = 0$) from the fiducial scenario. In both Figs 2 and 3, the grey shaded areas correspond to the ratio of the ΛCDM non-linear matter power spectrum computed with the HALOFIT package (Smith et al. 2003) within the CAMB code by setting all cosmological parameters to their fiducial *Planck* values except for σ_8 which is allowed to vary within its 2σ confidence interval (according to Ade et al. 2013). In other words, the grey shaded areas provide a visual estimate of the discriminating power of presently available cosmological data. This is clearly just a rough indicative estimate since we are varying only one parameter, but still provides a quantitative idea of how the differences among the various models compare with deviations allowed by present observational uncertainties on standard cosmological parameters.

These results clearly show that $f(R)$ MG models are strongly degenerate with massive neutrinos, such that a combination of both extensions of the standard cosmological model might prevent or significantly dim the prospects to constrain any of them through a direct observational determination of the matter power spectrum at low redshifts, unless an independent measurement of the total neutrino mass from particle physics experiments becomes available. This conclusion extends the previous results of He (2013) (based on CMB observations at high-z) and the recent analysis of Motohashi et al. (2013) (which combines both high-z CMB data and low-z linear power spectrum measurements) to the low-z non-linear regime of structure formation by employing for the first time specifically designed N-body simulations that allow us to consistently evolve $f(R)$ MG cosmologies in the presence of massive neutrinos. This degeneracy therefore poses a further theoretical limitation on the constraints that can be inferred on cosmological parameters and extended cosmological models from accurate observational determinations of the matter power spectrum, besides the widely discussed degeneracy with the uncertain effects of baryonic physical processes at small scales, such as e.g. the feedback from active galactic nuclei (AGN; see e.g. Semboloni et al. 2011; Puchwein et al. 2013 for an estimate of the biasing effects of AGN feedback mechanisms on the determination of standard cosmological parameters and on the peculiar signatures of $f(R)$ MG models, respectively). Nonetheless, as one can see by comparing the different panels of Fig. 3, the redshift evolution of the power spectrum might provide a way to disentangle the two effects if sufficiently precise observational measurements of the matter power spectrum up to a comoving

wavelength of $k \approx 10\,h\,\mathrm{Mpc}^{-1}$ can be obtained for different values of $z \lesssim 1.3$.

We defer a more complete survey of other $f(R)$ cosmologies to a follow-up paper, as in this work we are mainly interested in assessing the degeneracy between $f(R)$ gravity and massive neutrinos at a semi-quantitative level. However, it is natural to expect that milder realizations of $f(R)$ theories – such as e.g. $\bar{f}_{R0} = \{-1 \times 10^{-5}, -1 \times 10^{-6}\}$ – will result in a similar kind of degeneracy with lower values of the neutrino mass and might therefore be even more difficult to disentangle observationally.

In order to compare directly the suppression effect of massive neutrinos in the two different theories of gravity, in Fig. 4 we display the ratio of the matter power spectra in the massive and massless neutrino cases for GR (solid lines) and $f(R)$ (dashed lines) cosmologies, for the same redshifts displayed in Figs 2 and 3. As one can see in the plots, the relative suppression induced by massive neutrinos is roughly the same for GR and $f(R)$ gravity, with some small deviations at the most non-linear scales, which can be ascribed to the different stage of evolution of the LSS in which massive neutrinos evolve for the different cosmologies. This result suggests that a sufficiently accurate estimate of the full non-linear matter power spectrum in models that combine $f(R)$ gravity with a massive neutrino background might be obtained by applying fitting functions of the neutrino suppression obtained with standard GR simulations on top of the non-linear matter power spectrum computed with pure $f(R)$ runs. However, such an approximation should be properly tested for a wider range of neutrino masses and $f(R)$ gravity realizations before being considered sufficiently robust.

To conclude our investigation of the matter power spectrum, we have computed the growth factor of density perturbations at three different scales $k = 0.1\,,\,0.5\,,\,1.0\,h\,\mathrm{Mpc}^{-1}$ by computing the square root of the ratio of the power spectrum amplitudes at the various snapshots of our simulations suite to the amplitude at $z = 0$. The results of this procedure are displayed in the three panels of Fig. 5, where we plot the ratio of the growth factor of the different models under investigation to the fiducial case of GR and massless neutrinos. As one can see in the figures, GR and $f(R)$ models have (as expected) an opposite trend in the growth of density perturbations as compared to the fiducial case at all scales. Interestingly, while at linear and mildly non-linear scales ($k = 0.1$; $0.5\,h\,\mathrm{Mpc}^{-1}$) the hierarchy of the models follows the expected linear trend at all redshifts, at the most non-linear scales ($k = 1\,h\,\mathrm{Mpc}^{-1}$) the different models are found to be more entangled at low redshifts, while the growth factor slope at high redshifts shows again the expected linear behaviour. This highlights how the complex non-linear interplay of the different gravity and neutrinos models produces non-trivial effects on the evolution of density perturbations at very small scales. A detailed study of such highly non-linear effects would require much higher resolution simulations than those available to our present suite, and we defer it to future works.

5.2 The halo mass function

For all the simulations of our sample, we have identified dark matter haloes by means of a friends-of-friends (FoF) algorithm with linking length $\ell = 0.2 \times \bar{d}$, where $\bar{d}$ is the mean interparticle separation. In this case, we have considered only CDM particles in the linking procedure, such that the obtained haloes do not include neutrino particles. This is to avoid spurious mass contamination arising from unbound neutrino particles (see e.g. Castorina et al. 2013; Costanzi et al. 2013). We emphasize that the contribution of massive neutrinos to the total mass of the dark matter halo is negligible for the

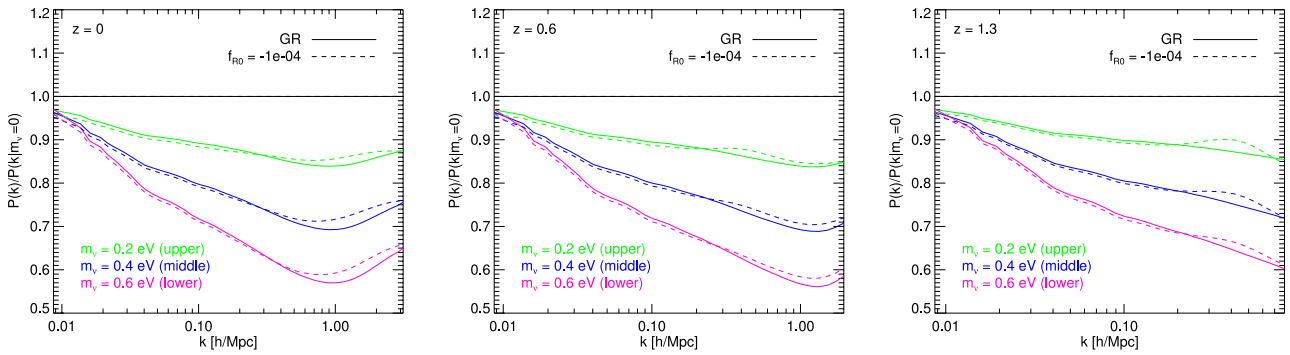

Figure 4. The matter power spectrum suppression due to the presence of massive neutrinos in both GR (solid lines) and $f(R)$ (dashed lines) models as compared to the massless neutrino case at different redshifts: $z = 0$ (left), $z = 0.6$ (middle), and $z = 1.3$ (right).

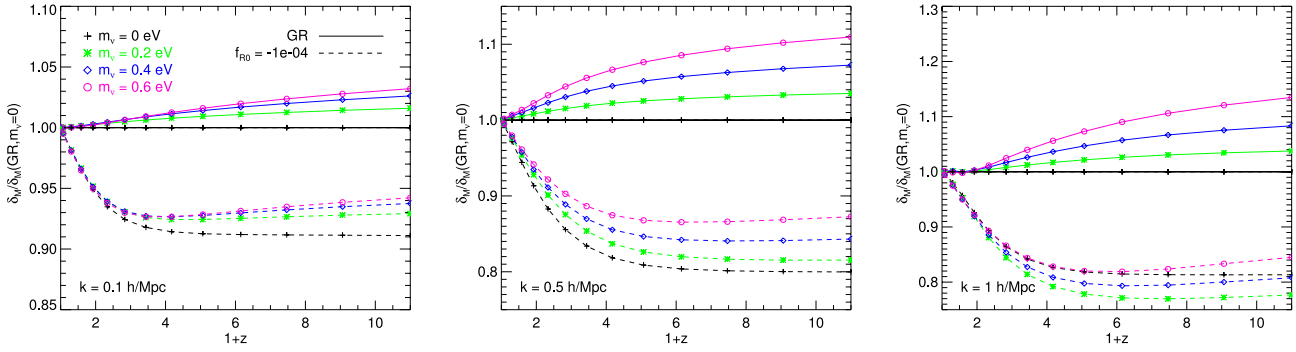

Figure 5. The evolution of the matter density perturbations amplitude as a function of redshift normalized to the fiducial model at three different scales in the linear ($k = 0.1\,h\,\mathrm{Mpc}^{-1}$, left), mildly non-linear ($k = 0.5\,h\,\mathrm{Mpc}^{-1}$, middle), and non-linear ($k = 1\,h\,\mathrm{Mpc}^{-1}$, right) regimes of structure formation.

masses considered in this paper, as it was recently verified with N-body simulations in the context of the standard ΛCDM cosmology (Villaescusa-Navarro et al. 2011a, 2013a; LoVerde & Zaldarriaga 2013). We have directly checked that this result still holds also for $f(R)$ gravity models by comparing spherical overdensity halo masses with and without the contribution of massive neutrino particles in our $f(R)$ simulation with the largest neutrino mass (fR-nu0.6), finding deviations below 1 per cent over the whole mass range of the halo sample. Furthermore, for each FoF halo, we have identified its gravitationally bound substructures by means of the SUBFIND algorithm (Springel et al. 2001), and we associate to each FoF halo the virial mass M_{200} of its primary substructure computed as the mass of a spherical region centred on the particle with the minimum potential of the halo enclosing a mean overdensity 200 times larger than the critical density of the universe. With this catalogue of haloes at hand, we have computed the HMF by binning the haloes of each cosmological simulation in 10 logarithmically equispaced mass bins over the mass range $3.0 \times 10^{13} - 1.0 \times 10^{15}$ $\mathrm{M}_{\odot}\, h^{-1}$, where the lower mass bound is given by the minimum halo mass resolved by the FoF algorithm for the fiducial cosmology.

In Fig. 6, we plot for different redshifts the ratio of the spherical overdensity HMF obtained with SUBFIND for GR gravity with different values of the total neutrino mass to the fiducial case of GR and massless neutrinos. As expected, and consistently with previous findings (see e.g. Brandbyge et al. 2010; Marulli et al. 2011; Ichiki & Takada 2012; Castorina et al. 2013; Costanzi et al. 2013; Villaescusa-Navarro et al. 2013a), the presence of massive neutrinos significantly reduces the abundance of haloes over the whole mass range allowed by our sample, with the suppression being more severe for more massive haloes and for larger values of the neutrino mass. This effect shows a rather weak redshift dependence for $z \lesssim 1.3$.

We now consider the combined effect of massive neutrinos and of an $f(R)$ MG theory on the HMF. In Fig. 7, we display the ratio of the halo abundance for the $\bar{f}_{R0} = -1 \times 10^{-4}$ MG model discussed in this paper with different values of the neutrino mass as compared to the fiducial cosmology with GR and massless neutrinos. As the plots show, the $f(R)$ model alone significantly enhances the abundance of haloes, in particular at large masses. On the other hand, when MG is associated with a non-vanishing neutrino mass, this enhancement is significantly reduced over the whole mass range available within our sample, with the largest neutrino mass included in our investigation ($\Sigma_i m_{\nu_i} = 0.6$ eV) even resulting in an overall suppression of the halo abundance at all masses and at all redshifts.

Analogously to what we displayed in the power spectrum ratio plots above, in Figs 6 and 7 the grey shaded areas correspond to the mass function ratios obtained by computing the HMF through the standard Jenkins fitting formula (Jenkins et al. 2001) for the *Planck* cosmological parameters of Table 2 but allowing σ_8 to vary within its 2σ confidence interval. This region therefore provides a visual indication of the present discriminating power of observational determinations of the halo abundance at different redshifts with respect to the range of cosmological models discussed in this work.

The results show again that also for the abundance of dark matter haloes there is a strong degeneracy between the effects of a modification of gravity and of a non-vanishing neutrino mass, such that a suitable combination of these two independent extensions of the standard cosmological model can result in an overall abundance of dark matter haloes hardly distinguishable from that of the standard fiducial ΛCDM cosmology with massless neutrinos.

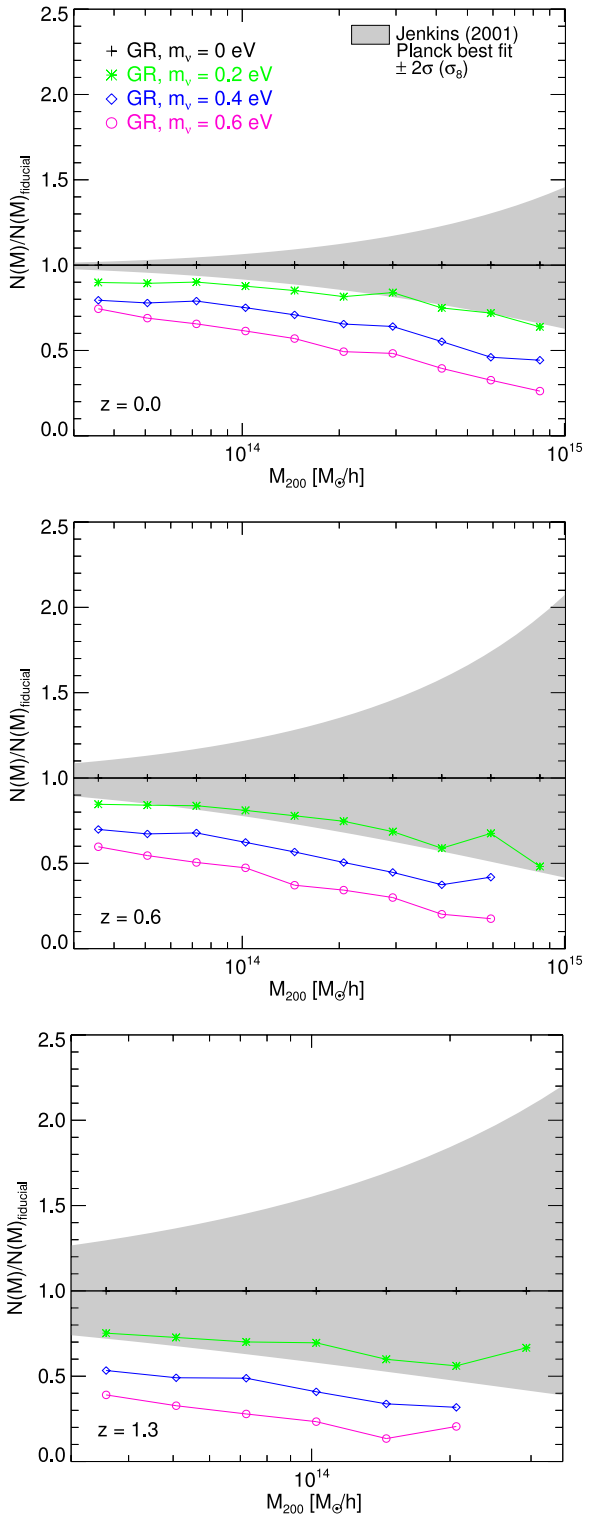

Figure 6. The ratio of the spherical overdensity HMF in GR simulations with different neutrino masses as compared to the fiducial case of GR and massless neutrinos. Different panels refer to different redshifts as for Figs 2 and 3. The grey shaded areas correspond to the variation of the HMF obtained with the standard Jenkins fitting formula (Jenkins et al. 2001) by varying σ_8 within its 2σ confidence interval according to the latest *Planck* cosmological constraints (Ade et al. 2013).

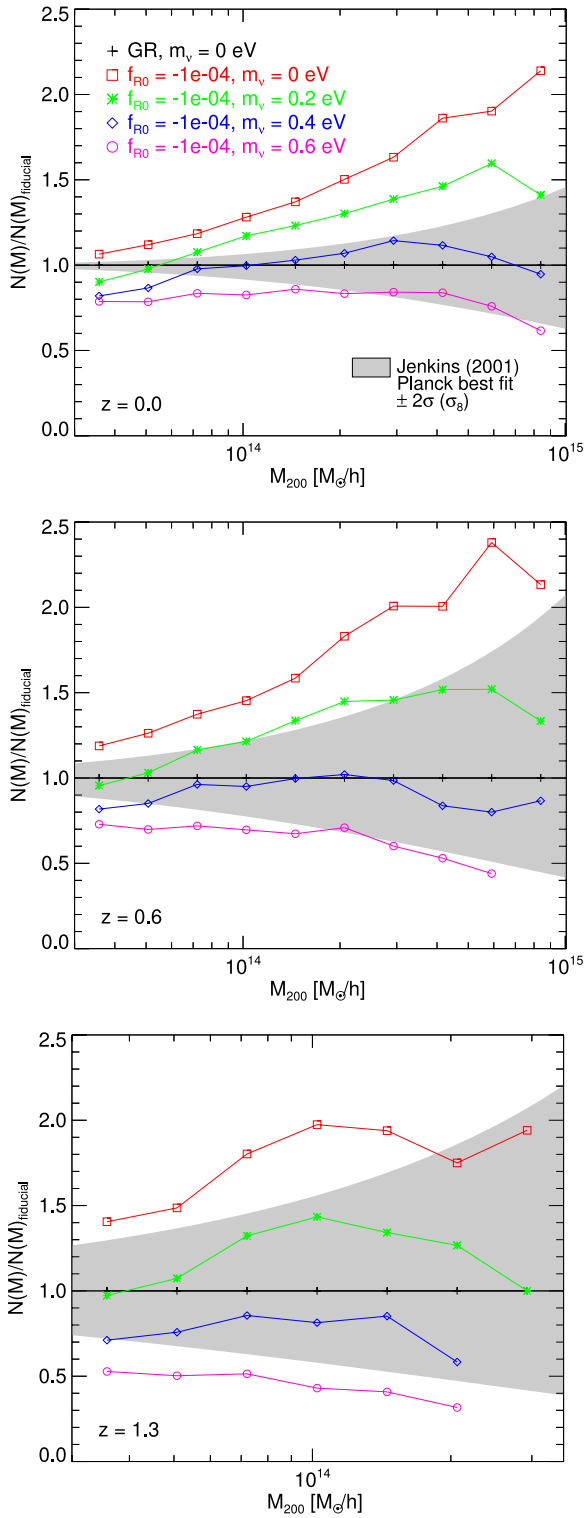

Figure 7. As Fig. 6, but for the combined simulations of $f(R)$ gravity and massive neutrinos.

In analogy to what we have done above for the non-linear matter power spectrum, in Fig. 8, we show the suppression effect on the HMF of massive neutrinos of different masses as compared to the massless case in the GR (solid lines) and $f(R)$ (dashed lines) simulations. Also in this case, one can see that the neutrino-induced suppression is roughly the same in the two theories of gravity, even though at low redshifts the $f(R)$ model systematically shows a slightly lower suppression than the GR case. This again appears to be related to the more evolved large-scale distribution that characterizes $f(R)$ cosmologies as compared to GR at low redshifts, which makes the impact of massive neutrinos slightly less effective.

Finally, in Fig. 9, we display the relative abundance – as compared to the fiducial model – of haloes above a given mass threshold M as a function of redshift and halo mass, for the same three redshifts considered in previous figures and for three values of the threshold mass $M = \{10^{13}, 10^{14}, 10^{15}\}\ \mathrm{M}_{\odot}\, h^{-1}$. Therefore, this ratio shows the evolution of halo counts as a function of redshift in the different models. From the left-hand panel, we notice that massive neutrinos always suppress halo number counts at all masses and redshifts, while the massless neutrinos $f(R)$ model (red curve in the right-hand panel) always shows a higher number counts than its GR counterpart. Also here, it is interesting to notice that the fiducial model lies in between the $\Sigma_i m_{\nu_i} = 0.2$ and the 0.4 eV cases for all mass thresholds and for all redshifts, thereby confirming the degeneracy observed in all the other statistics discussed so far.

5.3 Halo-matter bias

Both galaxies and dark matter haloes are biased tracers of the underlying matter distribution. In this section, we focus on the bias between the spatial distribution of dark matter haloes and that of the underlying matter for the different cosmological models considered in this paper. We compute the bias as the ratio of the halo-matter cross-power spectrum, $P_{\rm hm}$, to the matter autopower spectrum $P_{\rm mm}$

$$b_{\rm hm}(k) = \frac{P_{\rm hm}(k)}{P_{\rm mm}(k)}. \tag{11}$$

We have used this estimator for the bias since it does not suffer from shot-noise (Dekel & Lahav 1999; Smith, Scoccimarro & Sheth 2007; Baldauf et al. 2010, 2013; Hamaus et al. 2010). Our halo catalogue consists of FoF haloes with masses above $2.3 \times 10^{13}\, h^{-1}\mathrm{M}_{\odot}$. A detailed description of the method used to compute the power spectra can be found in Villaescusa-Navarro et al. (2013b).

In Fig. 10, we show the bias of each cosmological model normalized to the bias of the GR massless neutrino model. Similarly to previous figures, we show the results at $z = 0$ (top), $z = 0.6$ (middle), and $z = 1.3$ (bottom). In both GR and $f(R)$ cosmological models, the effect of massive neutrinos goes in the same direction, enhancing the bias of dark matter haloes at all scales. This is due to the fact that massive neutrinos induce a suppression on the matter power spectrum which has the effect that dark matter haloes of a given mass are rarer in a massive neutrino cosmology in comparison with a universe with massless neutrinos. Therefore, we expect the bias of objects of the same mass to be higher in a cosmological model with massive neutrinos.

In the GR cosmological model, we find that massive neutrinos induce a significant scale-dependent bias on large scales as found in Villaescusa-Navarro et al. (2013b) and Castorina et al. (2013). This is clearly seen in the GR $\Sigma_i m_{\nu_i} = 0.6$ eV model (solid magenta line). In contrast, we find that for the $f(R)$ cosmological models incorporating massive neutrinos the large-scale bias does not exhibit any significant scale dependence, thereby recovering the flat behaviour that characterizes the standard scenario. We will explore this point in further detail in a follow-up paper by using a larger suite of N-body simulations.

At $z = 0$, the bias of the $f(R)$ MG model with $\Sigma_i m_{\nu_i} = 0.4$ eV only differs from that of the fiducial GR massless neutrino model

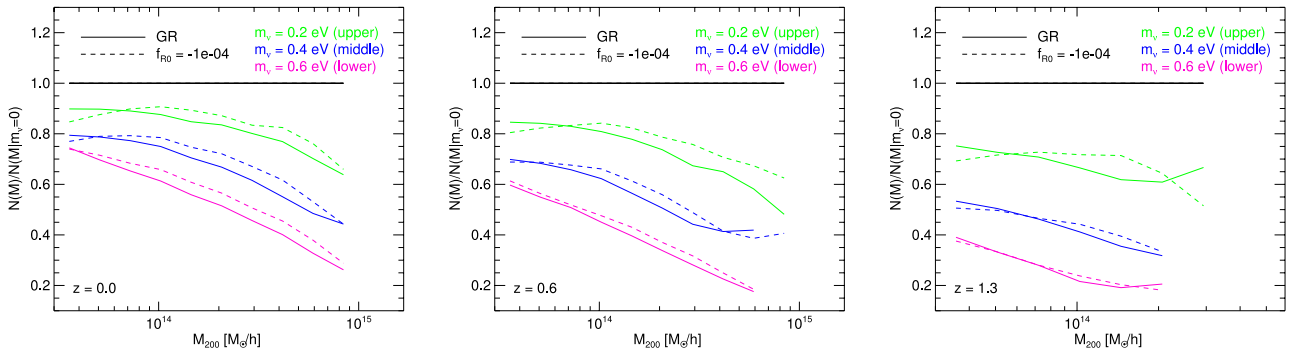

Figure 8. The ratio of the spherical overdensity HMF for the different neutrino masses with respect to the massless case for a GR (solid lines) and $f(R)$ (dashed lines) theory of gravity at different redshifts: $z = 0$ (left), $z = 0.6$ (middle), and $z = 1.3$ (right).

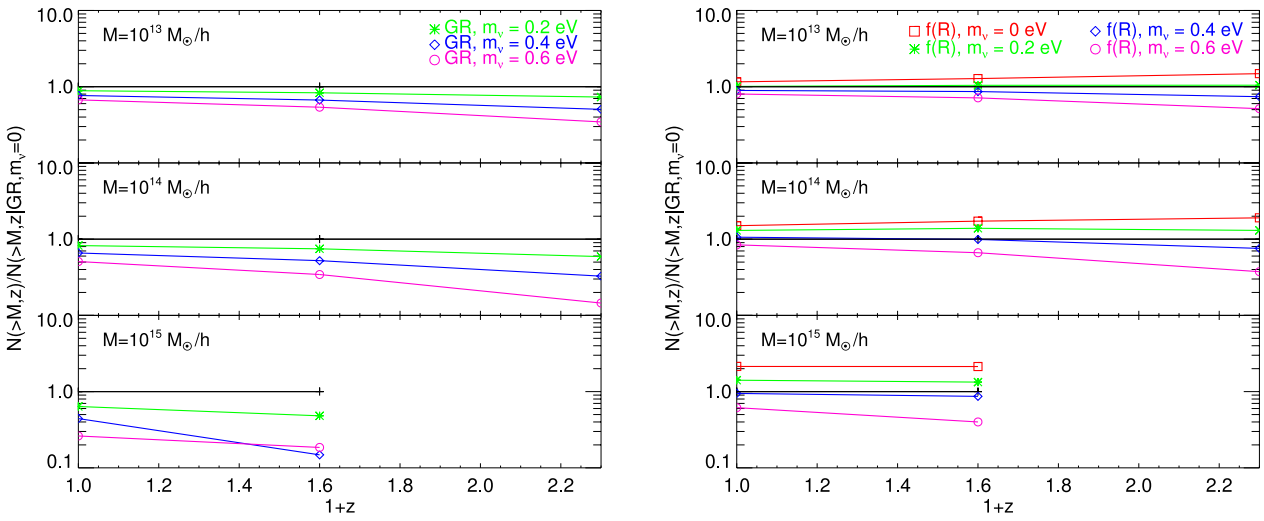

Figure 9. The ratio of halo number counts above three different mass thresholds with respect to the fiducial model as a function of redshift for the GR (left) and the $f(R)$ (right) simulations with different neutrino masses.

by less than 3 per cent at all scales. At $z = 0.6$, the bias of the 0.4 eV $f(R)$ MG model only departs by less than a 5 per cent from the bias of the fiducial model. Larger differences among the above two models arise at $z = 1.3$ (∼15 per cent), although these differences still do not depend on scale at any redshift.

Whereas at $z = 0.6$, the bias of the $f(R)$ MG model with $\Sigma_i m_{\nu_i} = 0.2$ eV is almost perfectly (below 2 per cent) degenerate with the massless neutrinos GR cosmology, larger departures occur at $z = 0$ (∼5 per cent) and $z = 1.3$ (∼10 per cent). Also in this case, we find that the differences between the above two models does not depend on scale at any redshift.

Therefore, we conclude that the degeneracies we find for the matter power spectrum and the HMF between $f(R)$ MG models with massive neutrinos and the massless GR cosmology also show up in the halo bias. The degeneracy is almost perfect at redshifts $z = 0$ and 0.6, while it is slightly broken at $z = 1.3$. Interestingly, the differences we find for the bias between the $f(R)$ MG model with $\Sigma_i m_{\nu_i} = 0.4$ eV neutrinos and the massless neutrinos GR cosmology does not depend on the scale at any redshift.

6 CONCLUSIONS

Identifying and computing the characteristic signatures of extended cosmological models beyond the standard ΛCDM scenario represents a necessary step in order to fully exploit the unprecedented accuracy of several present and future observational initiatives. On one hand, such an identification will provide a robust interpretative framework for possible (and somewhat hoped for) observational features in tension with the predictions of the standard cosmological scenario; on the other hand, the quantitative estimation of the deviations expected in different observables as a consequence of specific extensions of the standard model allows an assessment of the effective discriminating power of present and future data sets with respect to such extended scenarios. Given the high level of accuracy and the wide range of scales involved, a comparison between theoretical predictions and observational data cannot be restricted to the background expansion history and the linear regime of structure formation, but needs to be self-consistently extended to the fully non-linear regime, thereby requiring the use of large dedicated numerical simulations.

In recent years, a wide number of specifically designed numerical tools have been developed with this aim, allowing us to predict the impact of several extended cosmological models on various observables. However, most numerical implementations have been designed to investigate one specific class of extended cosmologies at a time, without allowing for the possibility that the real universe might deviate from our standard model in more than one aspect at the same time. In other words, while detailed and robust predictions at the non-linear level are starting to be produced for individual scenarios that extend the minimal ΛCDM cosmology by challenging

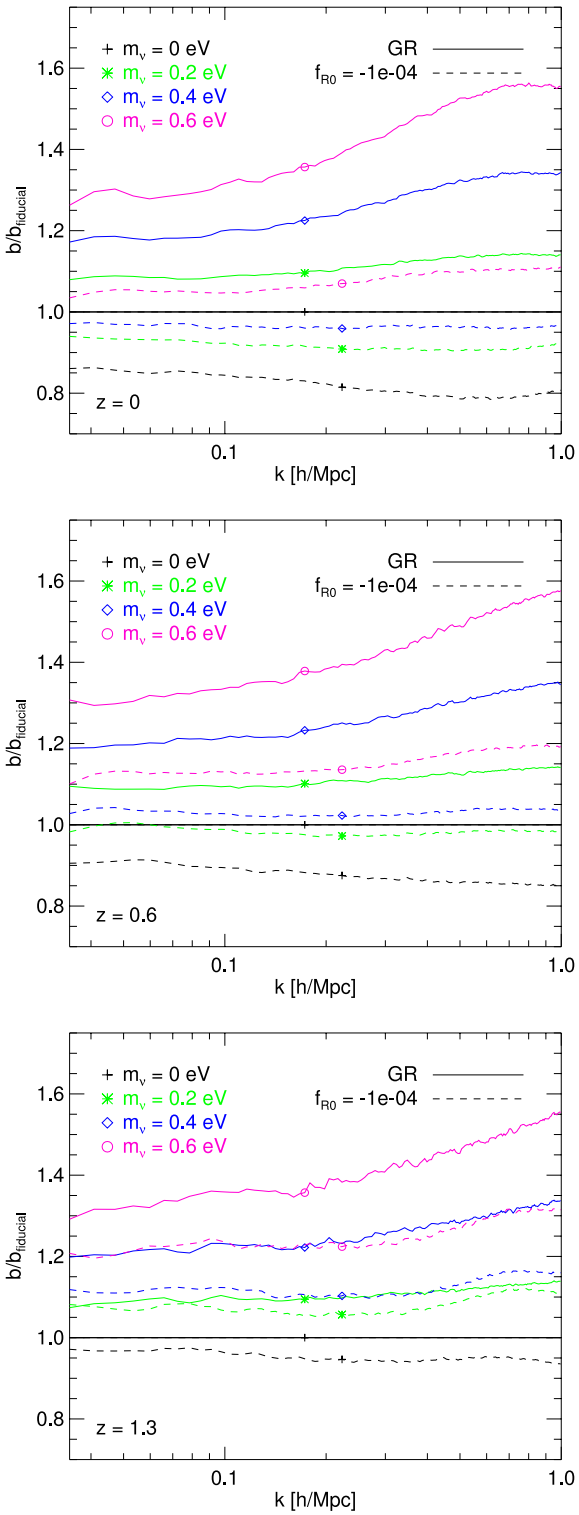

Figure 10. The ratio of the halo bias for different neutrino masses in the GR and $f(R)$ cosmologies considered in this paper (solid and dashed curves, respectively) over the bias obtained in the fiducial run with GR and massless neutrinos. The three panels refer to different redshifts ($z = \{0\,,\,0.6\,,\,1.3\}$) as for the previous figures.

only one among its fundamental assumptions (be it the nature of the DE, the theory of gravity, the statistical properties of the primordial density field, or the composition of the Dark Matter fraction), these predictions usually require that all the other standard assumptions still hold, thereby discarding possible degeneracies among different and independent extensions of the standard model.

In this paper – which is the first in a series of works devoted to the investigation of the possible degeneracies among different and independent extensions of the standard cosmological model – we have gone beyond this oversimplified setup by including for the first time in the same numerical treatment the combined effects of a modified theory of gravity [in the form of an $f(R)$ model] and of a cosmological background of massive neutrinos. To this end, we have combined the recent MG-GADGET implementation of $f(R)$ gravity by Puchwein et al. (2013) with the massive neutrinos algorithm developed by Viel et al. (2010), allowing us to perform the first cosmological simulations of massive neutrinos in the context of an underlying $f(R)$ cosmology.

With such code at hand, we have run a suite of intermediate-resolution simulations of structure formation, and we have investigated the impact of this twofold extension of the standard model on three basic statistics of the large-scale dark matter distribution, namely the non-linear matter power spectrum, the HMF, and the halo bias. Interestingly, our results have revealed a very strong degeneracy between the observational signatures of $f(R)$ gravity and those of a massive neutrino background in all these three statistics, thereby confirming that the conservative assumption of testing different extensions of the standard model on an individual basis is clearly too restrictive and might lead to significant misinterpretations of present and future observational data. In particular, our investigation most remarkably shows that a suitable combination of the characteristic parameters of $f(R)$ gravity and of the total neutrino mass, which would individually determine very significant deviations from the standard predictions in all three observables, results hardly distinguishable from the expectations of the standard cosmology. As a consequence, the discriminating power of present and future observational constraints based on these statistics (or on any combination of them) with respect to a possible modification of the laws of gravity or to a non-negligible value of the neutrino mass might be strongly weakened if the two effects are simultaneously at work. Similarly, null tests of the standard cosmological picture based on the same three observables might not be able to conclusively exclude any of the two individual extended scenarios since their combination provides nearly indistinguishable predictions as compared to the reference model.

More specifically, we have computed the deviation with respect to the fiducial scenario (i.e. ΛCDM with massless neutrinos) of the total non-linear matter power spectrum for a range of simulations including both separate realizations of $f(R)$ gravity and non-negligible neutrino masses, and their combination. As expected, the former simulations show significant deviations with respect to the fiducial case, in full agreement with previous results in the literature. Massive neutrinos determine a scale- and redshift-dependent suppression of the matter power spectrum at both linear and non-linear scales, with a maximum deviation from the massless case at $k \sim 1\,h\,\mathrm{Mpc}^{-1}$ and at $z = 0$, reaching about 45 per cent for the case of a total neutrino mass $\Sigma_i m_{\nu_i} = 0.6$ eV, which is the largest value considered in this work. On the other hand, $f(R)$ MG determines an enhancement of the non-linear power at similar scales, with a peak of about 55 per cent at $k \sim 0.6\,h\,\mathrm{Mpc}^{-1}$ and at $z = 0$ for the specific model assumed in this work ($f_{R0} = -1 \times 10^{-4}$). However, when the two effects are simultaneously included in the simulations, their combined impact on the matter power spectrum is strongly suppressed with respect to the separate individual realizations. More quantitatively, the combination of our $f(R)$ MG cosmology with a neutrino background with total mass $\Sigma_i m_{\nu_i} = 0.4$ eV does not

deviate more than ∼10 per cent in the non-linear matter power spectrum at $z = 0$ from the fiducial model over the whole range of scales available within our simulations suite. The combined deviation is slightly larger for higher redshifts, but never exceeds ∼15 per cent up to $z = 1.3$. These results show very clearly the significant level of degeneracy between these two independent extensions of the standard cosmological model.

Similarly, we have computed the HMF for all the simulations of our suite and compared the abundance of collapsed structures in all the runs with the fiducial case of standard gravity and massless neutrinos. Again, the two separate extensions of the standard cosmological model show very significant deviations in the abundance of structures at all redshifts, with the massive neutrinos determining a significant suppression of the HMF, especially at large masses, while our realization of $f(R)$ MG tends to produce a much larger number of haloes, with an enhancement of the HMF up to a factor ∼2 for the largest masses available in our simulations at $z = 0$. Also in this case, however, when the two extensions are simultaneously included in the numerical integration, their overall combined effect is much weaker than for the separate cases just described. Interestingly, the same combination of parameters that are the most degenerate with the fiducial model for what concerns the non-linear matter power spectrum is found to provide also the most degenerate mass function, thereby preventing the possibility of using a combination of such two observables in order to disentangle the different scenarios.

Finally, we have performed the same type of comparison for a third basic statistics of the large-scale matter distribution: the halo-matter bias. Also in this case, both $f(R)$ MG and massive neutrinos determine significant deviations in the halo bias as a function of scale and redshift. Consistently with previous studies, we find that massive neutrinos introduce a clear scale dependence of the halo bias as compared to the almost scale-independent behaviour of the fiducial cosmology, with larger scales showing a lower value of the bias, and with a slope of the scale dependence that increases with the total neutrino mass. We find that a similar phenomenon occurs also for $f(R)$ MG, although with a much weaker amplitude and an opposite trend of the scale dependence. Again, when the two extensions of the standard cosmological model are combined in the same simulations, the impact on the bias is significantly reduced, both in its overall amplitude and in its scale dependence. Also in this case, at $z = 0$ the most effective suppression of the predicted deviation occurs for the same combination of parameters that maximally suppress the deviation in the other statistics. However, the combined bias seems to show a more significant redshift evolution as compared to the previous observables, thereby providing a possible way to break the (otherwise ubiquitous) degeneracy among the different cosmological models. This possibility will be further investigated in more detail in a follow-up work.

To conclude, we have presented in this work the first cosmological simulations that combine the effects of $f(R)$ MG and of a cosmological background of massive neutrinos. Our investigation is part of a long-term programme aimed at studying and quantifying possible degeneracies between different and mutually non-exclusive extensions of the standard ΛCDM cosmological scenario. In this first study, we have demonstrated that assessing the expected features arising in different observables as a consequence of a specific extension of the standard cosmological framework without properly taking into account possible degeneracies with other independent extensions might lead to significantly overestimating the constraining power of present and future observational data sets. In particular, we have shown that with a suitable (and not unreasonable) choice of parameters, a combination of $f(R)$ MG and massive neutrinos might result in a large-scale matter distribution which is hardly distinguishable from a standard ΛCDM cosmology in several of its basic statistics.

Therefore, our results suggest an intrinsic theoretical limit to the effective discriminating power of present and future cosmological observations in the absence of an independent determination of the masses of neutrinos coming from particle physics experiments.

ACKNOWLEDGEMENTS

We acknowledge financial contributions from contracts ASI/INAF I/023/12/0, by the PRIN MIUR 2010–2011 'The dark Universe and the cosmic evolution of baryons: from current surveys to Euclid' and by the PRIN INAF 2012 'The Universe in the box: multiscale simulations of cosmic structure'. MB is supported by the Marie Curie Intra European Fellowship 'SIDUN' within the 7th Framework Programme of the European Commission. FVN and MV are supported by the ERC Starting Grant 'cosmoIGM'. EP and VS acknowledge support by the Deutsche Forschungsgemeinschaft through Transregio 33, 'The Dark Universe'. EP also acknowledges support by the ERC grant 'The Emergence of Structure during the epoch of Reionization'. The numerical simulations presented in this work have been performed and analysed on a number of supercomputing infrastructures: the MareNostrum3 cluster at the BSC supercomputing centre in Barcelona (through the PRACE Tier-0 grant 'SIBEL1'); the Hydra cluster at the RZG supercomputing centre in Garching; the COSMOS Consortium supercomputer within the DiRAC Facility jointly funded by STFC, the Large Facilities Capital Fund of BIS and the University of Cambridge; the Darwin Supercomputer of the University of Cambridge High Performance Computing Service (http://www.hpc.cam.ac.uk/), provided by Dell Inc. using Strategic Research Infrastructure Funding from the Higher Education Funding Council for England.

REFERENCES

Abazajian K. N. et al., 2009, ApJS, 182, 543
Abbott T. et al., 2005, preprint (arXiv:astro-ph/0510346)
Ade P. et al., 2013, preprint (arXiv:1303.5076)
Agarwal S., Feldman H. A., 2011, MNRAS, 410, 1647
Ahn C. P. et al., 2013, preprint (arXiv:1307.7735)
Amendola L., 2000, Phys. Rev. D, 62, 043511
Amendola L., Baldi M., Wetterich C., 2008, Phys. Rev. D, 78, 023015
Armendariz-Picon C., Mukhanov V. F., Steinhardt P. J., 2001, Phys. Rev. D, 63, 103510
Baldauf T., Smith R. E., Seljak U., Mandelbaum R., 2010, Phys. Rev. D, 81, 063531
Baldauf T., Seljak U., Smith R. E., Hamaus N., Desjacques V., 2013, Phys. Rev. D, 88, 083507
Baldi M., 2011, MNRAS, 411, 1077
Baldi M., 2012, Phys. Dark Universe, 1, 162
Baldi M., 2013, MNRAS, 428, 2074
Batista R., Pace F., 2013, J. Cosmol. Astropart. Phys., 06, 044
Bennett C. et al., 2013, ApJS, 208, 20
Bird S., Viel M., Haehnelt M. G., 2012, MNRAS, 420, 2551
Blake C. et al., 2011, MNRAS, 418, 1707
Bode P., Ostriker J. P., Turok N., 2001, ApJ, 556, 93
Brandbyge J., Hannestad S., 2009, J. Cosmol. Astropart. Phys., 5, 2
Brandbyge J., Hannestad S., 2010, J. Cosmol. Astropart. Phys., 1001, 021
Brandbyge J., Hannestad S., Haugbølle T., Thomsen B., 2008, J. Cosmol. Astropart. Phys., 8, 20
Brandbyge J., Hannestad S., Haugbølle T., Wong Y. Y. Y., 2010, J. Cosmol. Astropart. Phys., 9, 14

Buchdahl H. A., 1970, MNRAS, 150, 1
Caldwell R., 2002, Phys. Lett. B, 545, 23
Castorina E., Sefusatti E., Sheth R. K., Villaescusa-Navarro F., Viel M., 2013, preprint (arXiv:1311.1212)
Cleveland B. T., Daily T., Davis R., Jr, Distel J. R., Lande K., Lee C. K., Wildenhain P. S., Ullman J., 1998, ApJ, 496, 505
Costanzi M., Villaescusa-Navarro F., Viel M., Xia J.-Q., Borgani S., Castorina E., Sefusatti E., 2013, J. Cosmol. Astropart. Phys., 12, 012
Cowan C. L., Jr, Reines F., Harrison F. B., Kruse H. W., McGuire A. D., 1956, Science, 124, 103
Creminelli P., D'Amico G., Norena J., Vernizzi F., 2009, J. Cosmol. Astropart. Phys., 0902, 018
Dekel A., Lahav O., 1999, ApJ, 520, 24
Dvali G., Gabadadze G., Porrati M., 2000, Phys. Lett. B, 485, 208
Farrar G. R., Peebles P. J. E., 2004, ApJ, 604, 1
Feng B., Wang X.-L., Zhang X.-M., 2005, Phys. Lett. B, 607, 35
Fogli G. L., Lisi E., Marrone A., Montanino D., Palazzo A., Rotunno A. M., 2012, Phys. Rev. D, 86, 013012
Forero D. V., Tórtola M., Valle J. W. F., 2012, Phys. Rev. D, 86, 073012
Hamaus N., Seljak U., Desjacques V., Smith R. E., Baldauf T., 2010, Phys. Rev. D, 82, 043515
He J.-h., 2013, Phys. Rev. D, 88, 103523
Hill G. J. et al., 2008, in Kodama T., Yamada T., Aoki K., eds, ASP Conf. Ser. Vol. 399, Panoramic Views of Galaxy Formation and Evolution. Astron. Soc. Pac., San Francisco, p. 115
Hu W., Sawicki I., 2007, Phys. Rev. D, 76, 064004
Ichiki K., Takada M., 2012, Phys. Rev. D, 85, 063521
Ivezic Z. et al., 2008, preprint (arXiv:0805.2366)
Jenkins A., Frenk C. S., White S. D. M., Colberg J. M., Cole S., Evrard A. E., Couchman H. M. P., Yoshida N., 2001, MNRAS, 321, 372
Joudaki S., 2012, Phys. Rev. D, 87, 083523
Kaiser N. et al., 2002, Proc. SPIE Int. Soc. Opt. Eng., 4836, 154
Laureijs R. et al., 2011, preprint (arXiv:1110.3193)
Lesgourgues J., Pastor S., 2006, Phys. Rep., 429, 307
Lewis A., Challinor A., Lasenby A., 2000, ApJ, 538, 473
Li B., Hellwing W. A., Koyama K., Zhao G.-B., Jennings E. et al., 2012a, MNRAS, 428, 743
Li B., Zhao G.-B., Teyssier R., Koyama K., 2012b, J. Cosmol. Astropart. Phys., 1201, 051
Llinares C., Mota D. F., Winther H. A., 2013, preprint (arXiv:1307.6748)
Loeb A., Weiner N., 2011, Phys. Rev. Lett., 106, 171302
Lombriser L., Koyama K., Zhao G.-B., Li B., 2012, Phys. Rev. D, 85, 124054
LoVerde M., Zaldarriaga M., 2013, preprint (arXiv:1310.6459)
Maccio' A. V., Ruchayskiy O., Boyarsky A., Munoz-Cuartas J. C., 2012, MNRAS, 428, 882
Marulli F., Carbone C., Viel M., Moscardini L., Cimatti A., 2011, MNRAS, 418, 346
Motohashi H., Starobinsky A. A., Yokoyama J., 2013, Phys. Rev. Lett., 110, 121302
Nicolis A., Rattazzi R., Trincherini E., 2009, Phys. Rev. D, 79, 064036
Oyaizu H., Lima M., Hu W., 2008, Phys. Rev. D, 78, 123524
Perlmutter S. et al., 1999, ApJ, 517, 565
Pogosian L., Silvestri A., 2008, Phys. Rev. D, 77, 023503
Puchwein E., Baldi M., Springel V., 2013, MNRAS, 436, 348
Ratra B., Peebles P. J. E., 1988, Phys. Rev. D, 37, 3406
Riemer-Sorensen S., Parkinson D., Davis T., Blake C., 2012, ApJ, 763, 89
Riess A. G. et al., 1998, AJ, 116, 1009
Ringwald A., Wong Y. Y. Y., 2004, J. Cosmol. Astropart. Phys., 12, 5
Schmidt B. P. et al., 1998, ApJ, 507, 46
Schmidt F., Lima M. V., Oyaizu H., Hu W., 2009, Phys. Rev. D, 79, 083518
Sefusatti E., Vernizzi F., 2011, J. Cosmol. Astropart. Phys., 1103, 047
Semboloni E., Hoekstra H., Schaye J., van Daalen M. P., McCarthy I. G., 2011, MNRAS, 417, 2020
Sheth R. K., Tormen G., 1999, MNRAS, 308, 119
Singh S., Ma C.-P., 2003, Phys. Rev. D, 67, 023506
Smith R. E. et al., 2003, MNRAS, 341, 1311
Smith R. E., Scoccimarro R., Sheth R. K., 2007, Phys. Rev. D, 75, 063512
Smoot G. F. et al., 1992, ApJ, 396, L1
Sotiriou T. P., Faraoni V., 2010, Rev. Mod. Phys., 82, 451
Springel V., 2005, MNRAS, 364, 1105
Springel V., White S. D. M., Tormen G., Kauffmann G., 2001, MNRAS, 328, 726
Starobinsky A. A., 1980, Phys. Lett. B, 91, 99
Viel M., Haehnelt M. G., Springel V., 2010, J. Cosmol. Astropart. Phys., 1006, 015
Viel M., Becker G. D., Bolton J. S., Haehnelt M. G., 2013, Phys. Rev. D, 88, 043502
Villaescusa-Navarro F., Miralda-Escudé J., Peña-Garay C., Quilis V., 2011a, J. Cosmol. Astropart. Phys., 6, 27
Villaescusa-Navarro F., Vogelsberger M., Viel M., Loeb A., 2011b, MNRAS, preprint (arXiv:1106.2543)
Villaescusa-Navarro F., Bird S., Peña-Garay C., Viel M., 2013a, J. Cosmol. Astropart. Phys., 3, 19
Villaescusa-Navarro F., Marulli F., Viel M., Branchini E., Castorina E., Sefusatti E., Saito S., 2013b, preprint (arXiv:1311.0866)
Wagner C., Verde L., Jimenez R., 2012, ApJ, 752, L31
Weinberg S., 2008, Cosmology. Oxford Univ. Press, Oxford
Wetterich C., 1988, Nucl. Phys. B, 302, 668
Wetterich C., 1995, A&A, 301, 321
Xia J.-Q. et al., 2012, J. Cosmol. Astropart. Phys., 6, 10
Zhao G.-B., Pogosian L., Silvestri A., Zylberberg J., 2009, Phys. Rev. D, 79, 083513
Zhao G.-B., Li B., Koyama K., 2011, Phys. Rev. D, 83, 044007
Zhao G.-B. et al., 2013, MNRAS, 436, 2038

This paper has been typeset from a TEX/LATEX file prepared by the author.